A surface force apparatus for nanorheology under large shear strain

Lionel Bureau

A surface force apparatus for nanorheology under large shear strain

Lionel Bureau*
Institut des Nanosciences de Paris, UMR 7588 CNRS-Université Paris 6, 140 rue de Lourmel, 75015 Paris, France
(Dated: April 23, 2007)

We describe a surface force apparatus designed to probe the rheology of a nanoconfined medium under large shear amplitudes (up to 500 μm). The instrument can be operated in closed-loop, controlling either the applied normal load or the thickness of the medium during shear experiments. Feedback control allows to greatly extend the range of confinement/shear strain attainable with the surface force apparatus. The performances of the instrument are illustrated using hexadecane as the confined medium.

I. INTRODUCTION

The surface force apparatus (SFA) has been developped more than thirty years ago to probe surface interactions through a direct determination of force *vs* separation between two atomically smooth surfaces [1, 2]. This technique, originally designed to measure forces between surfaces separated by an air gap, has then been extended to force measurements across liquids of various nature [3, 4]. It appears, from the large body of work done in the field, that many liquids, when confined down to molecular thickness, tend to order into layers parallel to the confining walls [5, 6, 7, 8, 9].

The existence of such a molecular layering of simple liquids is at the origin of a number of studies which addressed the question of the lubricating properties of nanoconfined fluids subjected to shear. To do so, different versions of the SFA have been designed, that allow for tangential displacements of one of the confining surface and shear force measurement. The studies performed with these friction devices focus either on the viscoelastic behavior of the confined fluid (*i.e.* on the response to small amplitude oscillatory shear) [10, 11] or on its frictional response when one of the surface is driven at constant speed in one direction [12, 14]. The following central result emerges: when confined to thicknesses on the order of five molecular diameters, liquids exhibit a finite yield stress and strongly non-newtonian flow properties. Moreover, such a solidlike behavior is most sensitive to the number of molecular layers between the walls [13, 14]. Maintaining a constant thickness, to within a few angstroms, of the medium during shear is thus of primary importance in these experiments.

Now, unavoidable mechanical imperfections of the instruments usually cause a slight non parallel motion of the surfaces, which typically results in thickness variations of 10–30 Å for a shear amplitude of 1 μm [15, 16]. For a weakly confined medium, of thickness $h \sim 100$ Å, the useful range of shear amplitude is thus limited to about 500 nm if one prescribes relative variations of h of less than a few percents. For a medium confined under a finite normal force applied through a spring of typical stiffness 300 N.m^{-1}, if one wants the above-mentioned non-parallelism to cause an "acceptable " load variation of, say, 5%, over a shear amplitude of 100 μm, the applied load must therefore be of at least 1 mN. Such a load level corresponds to strongly confined regimes where the thickness is typically 1–2 molecular layers.

Such conditions are not limiting as long as molecules of simple structure are confined, for which a shear amplitude of about 1 μm is enough to establish a steady-state regime. However, they may become more of a concern when investigating the rheological properties of more complex molecules like branched hydrocarbons or polymers, which exhibit transients corresponding to sliding distances of more than 100 μm [17, 18, 19].

To our knowledge, only two devices have been designed to allow for compensation of non-parallel motion and thus extend the range of shear amplitude and confinement to be investigated [8, 14, 15]. In the present paper, we describe a surface force apparatus with unique performances in terms of intersurface distance stability over large shear amplitudes. This apparatus relies on a well-established mechanical design [20], and uses multiple beam interferometry to determine the thickness of the confined medium. The particularity of the SFA presented here is to allow for time-resolved distance and normal force measurements that are used as input signals of a digital feedback loop. This enables us to operate the apparatus either at constant thickness or constant force during shear motion over up to 500 μm.

II. GENERAL DESCRIPTION

The general design of the surface force apparatus is given on Fig. 1. The medium of interest is confined between two molecularly smooth mica sheets glued on crossed cylindrical lenses, of radius of curvature 1 cm. The mechanical arrangement is very similar to that proposed by Parker and Christenson [20]: the SFA is made of an aluminium alloy cylindrical cell closed by a horizontal circular flange on which all the mechanical parts are mounted.

The lower mica surface is held at one end of a vertical spring, the other end of which is attached to a shaft that can be moved vertically (z axis) and horizontally (x axis).

*Electronic address: bureau@insp.jussieu.fr

Coarse vertical motion is produced by a miniature translation stage equipped with a stepper motor (Physik Instruments PI-M111.12s, total travel 15 mm, positioning accuracy 100 nm with controller PI-C630). Fine vertical approach of the surfaces is made by means of a hysteresis-free piezoactuator (PI-P753.11C and control electronics PI-E509.C3A) of 12 μm range, which includes a built-in capacitive sensor allowing for closed-loop operation with a positioning accuracy of 0.5 Å. Motion along the x axis is produced by a piezoactuator using the same technology but with a total travel of 500 μm (PI-P625.1CD and controller PI-E509.C1A).

The upper mica surface is held by a horizontal spring which serves as a shear force sensor.

The apparatus is placed on an active anti-vibration table (MOD-1M, Halcyonics GmbH, Germany), and the whole setup is housed in a home-made thermally regulated enclosure. Four low-noise ventilators are used to maintain forced convection inside the enclosure, where the temperature can be adjusted at ± 0.02°C in the range 10–45°C by means of a thermoelectric cooling/heating assembly controlled by a commercial PID unit (Super-Cool PR-59).

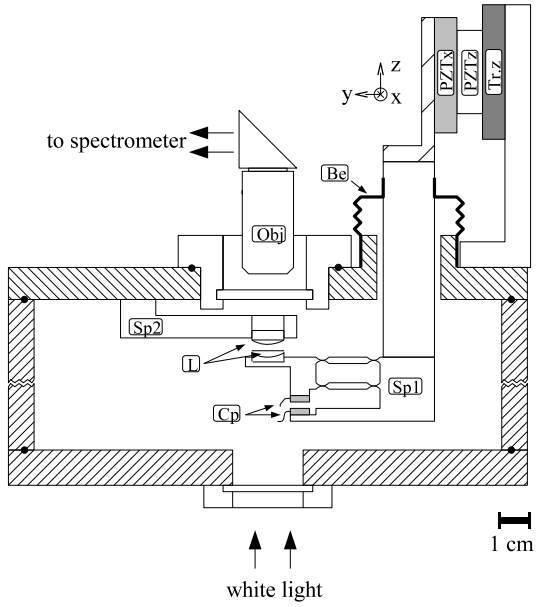

FIG. 1: Mechanical arrangement of the surface force apparatus. Two crossed cylindrical lenses (L) are mounted in springs (Sp1 and Sp2), the deflexion of which is measured by means of capacitive displacement sensors (Cp). The normal load spring (Sp1) is attached to a shaft that can be moved horizontally by means of a long travel piezoactuator (PZTx), and vertically *via* a two stage mechanism composed of a piezoactuator (PZTz) and a motorized translation stage (Tr.z). A rubber bellow (Be) is used to ensure air-tightness of the vessel while allowing for normal and tangential displacement of the shaft.

A. Force measurement

Both vertical and horizontal springs are deformable parallelograms with flexure hinges, each of them being precision-machined from one block of highly elastic aluminium alloy. Their respective stiffness are $K_N = 31000 \pm 800$ N.m^{-1} and $K_T = 28000 \pm 700$ N.m^{-1}, and their deflections are measured by means of capacitive displacement sensors with a 15 μm range (Physik Instruments D-015 with electronics E509.C3A) and a resolution of 1.5 pm/$\sqrt{\text{Hz}}$. This translates into a nominal force sensitivity, in both z and x directions, of $\sim$0.05 μN/$\sqrt{\text{Hz}}$ over a range of about 450 mN. In practice, the force sensitivity is limited by residual vibrations of the springs and is of ± 2 μN on a 100 Hz bandwidth. The maximum frequency at which force measurements can be performed is limited by the bandwidth of the electronics, namely 3kHz.

Note that in contrast with many surface force apparatuses, in which the normal load is deduced from the difference in the imposed displacement of the spring remote point and the displacement actually measured between the surfaces, our solution allows to perform force measurements independently of the distance determination.

B. Distance measurement

Intersurface distance measurement relies on multiple beam interferometry.

The Fabry-Perot cavity formed by the silvered mica sheets and the confined medium is shon with a collimated beam of white light produced by a 250W tungsten-halogen source (Lot-Oriel). Infrared radiation is filtered using a series of cold mirrors and water filters.

The region surrounding the point of closest distance between the cylindrical lenses is imaged on the entrance slit of a spectrograph using a long working distance microscope objective (VLD-MPA10, numerical aperture 0.23. Nachet, France,). The spatial resolution is diffraction limited and is of $\sim$1.5 μm.

The spectral position of the fringes of equal chromatic order (FECO) is determined with a half-meter imaging spectrometer (Acton spectra-pro 2500i) equipped with 3 gratings of 300, 600 and 1200 g/mm. A 16-bits 2D charge coupled device camera (PIXIS 400, Princeton Instruments, 1340$\times$ 400 pixels) is placed at the exit port of the spectrometer. With the 1200 g/mm grating, the spectral resolution is of 30 pm/pixel over a wavelength range of 40.2 nm. Good quality images of the spectrograph exit field are obtained with exposure times $t_{\text{exp}} \geq 20$ ms. The readout time of the full CCD array is of 280 ms, which yields a rate of about 3 frames per second for acquisition of the FECO along a spatial coordinate. If measurements of the FECO are made only at the point of closest distance, the readout time is that of a single row of pixel and drops to 17 ms, which, added to $t_{\text{exp}} \simeq 20$ ms, yields

a maximum rate of about 27 Hz for spectrum acquisition at a single location.

The distance between the mica surfaces is deduced from the FECO using a Labview-based implementation of fast spectral correlation (FSC) and multilayer matrix method (MMM), as introduced recently by Heuberger [21]. We briefly describe the protocol followed for distance measurements:

(i) the mica surfaces are brought into contact, a spectrum is acquired in the flattened contact zone, and the wavelengths λ_i of the transmission maxima are determined.

(ii) for the set of λ_i determined at mica-mica contact, we calculate, using the MMM, the transmissivity of the silver/mica/mica/silver layered medium for a range of plausible mica thickness d_{mica} (typically 10000–100000 Å, with 1 Å steps). We choose for d_{mica} the value that maximizes the function $T = \sum_i T_i$, where T_i is the transmissivity calculated at the wavelengths λ_i [21]. We finally calculate for this value of d_{mica} the transmissivity over the full experimental wavelength window in order to check if both the number and the position of the calculated transmission maxima are in agreement with the experimental spectrum. The time needed for the determination of d_{mica} is of a few seconds and is limited by the time for transmissivity calculation over the chosen thickness range.

(iii) the surfaces are separated by $\sim$ 1 mm, and the liquid is injected between them using a microsyringe.

(iv) the mica sheets are approached down to a separation of a few microns.

(v) the initial thickness of the liquid, d_0, is determined as in step *(ii)* above: we acquire a spectrum at the point of closest distance between the curved surfaces, locate the position of the transmission maxima, and calculate for these positions the transmissivity of the silver/mica/liquid/mica/silver multilayer for a range of plausible thickness (typically 0–50000 Å, with 10 Å steps), assuming that the refractive index of the liquid is the bulk one. Once again, the time needed to complete this step is limited by the transmissivity calculation over the range chosen for the trial values of d_0.

(vi) once d_0 is known, at each time t_i a new spectrum is acquired, the intersurface distance d_i is calculated as in step (v), with a range of plausible distance $d_{i-1} \pm \Delta d$, where d_{i-1} is the distance determined at time t_{i-1}. The time for transmissivity calculations using $\Delta d = 100$ Å and 1Å increments is on the order of 1 ms, and distance measurements can thus be performed at a rate limited only by spectra acquisition.

C. Data acquisition and feedback operation

Spectra are transfered to the host computer via its universal serial bus and treated immediatly to deduce the intersurface distance as described above. The signals corresponding to the normal and tangential forces and to the positions of the normal and tangential pizoactuators are measured by four digital multimeters (DMM 34401A, Agilent, $6^{1/2}$ digits). The synchronization output of the PIXIS camera is used to trigger the multimeters each time a spectrum has been acquired. Measurements from the DMMs are transfered to the host computer between each trigger event, *via* a GPIB-PCI card. Feedback operation can be performed using either the intersurface distance or the normal force signal as the input of a digital loop with proportional and integral control, which acts on the voltage of the normal piezoactuator. The gains of the loop were set as described in [22]: we first increase the proportional gain until oscillations are observed, lower it by a few percents from this value, then increase the integral gain in order to reduce the offset to setpoint.

III. PERFORMANCES

A. Sample preparation

Mica sheets are cleaved down to a thickness of 2–5 μm and cut into approximately 1 cm^2 squares by means of surgical scissors. This samples are put on a clean mica backing substrate with one angle lying on a thin teflon ribbon in order to allow for subsequent easy de-adhesion. The back side of the mica samples is evaporated with a 45nm-thick silver layer. The results presented hereafter have been obtained using glucose to glue the samples on the cylindrical lenses.

We demonstrate the performances of the apparatus using a linear alkane as a confined medium. We use anhydrous grade n-hexadecane (99+%, Sigma-Aldrich) filtered through a 0.2 μm teflon membrane. A droplet of the liquid (30–50 μL) is injected between the mica surfaces, a beaker containing phosphorus pentoxide is placed inside the vessel which is then sealed and left for thermal equilibration for 12h before starting experiments.

B. Layering under confinement

We first report the force-distance curve obtained when the surfaces are approached by driving the free end of the normal spring at a constant speed of 2Å.s^{-1}. Figure 2 clearly shows that the alkane exhibits layering under confinement, as seen from the 0.4–0.5 nm jumps in the intersurface distance, in agreement with previous studies of the same liquid [6, 15].

The present experimental setup allows for straightforward studies of dynamical effects which manifest when the fluid is confined at high enough velocities, and this without the need for post-analysis of recorded FECO patterns. This is illustrated on figure 3 where we have plotted two approach curves obtained at 0.2 and 5 nm.s^{-1}. It is seen on Fig. 3 that for thicknesses ranging from 1 to 4 nm, high velocity confinement leads to much less

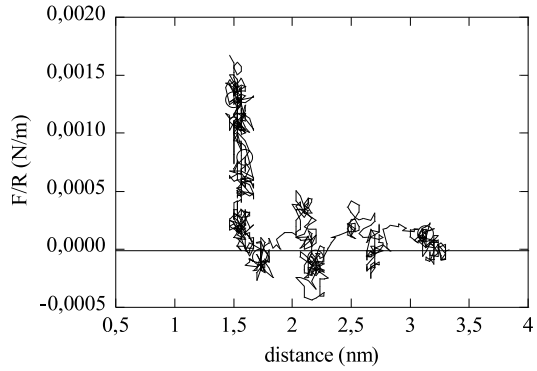

FIG. 2: Normalized force (normal load divided by radius of curvature) as a function of film thickness, for hexadecane confined between mica surfaces, at 24°C. The curve corresponds to the approach phase only. Data acquisition rate of 13 Hz.

molecular layering and to an upward shift of the force-distance profil, caracterizing the out-of-equilibrium response of the fluid.

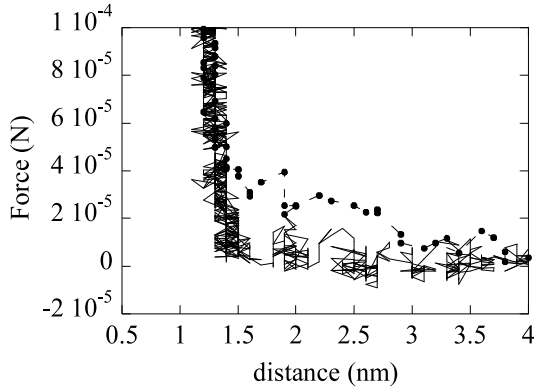

FIG. 3: Normal load as a function of hexadecane thickness for two approach velocities: 0.2 nm.s^{-1} (solid line) and 5 nm.s^{-1} (dashed line with symbols).

C. Large strain shear experiments

We now illustrate the shear capabilities of the instrument.

On figure 4, we show an experiment where a confined film of hexadecane is sheared at a speed of 5 μm.s^{-1} over a total sliding distance of 100 μm. This experiment was performed with a normal load setpoint of 185 μN and an acquisition rate of 25 Hz. Under such conditions, the normal load is found to settle at 178 μN during forward shear, and at 192 μN during backward motion (Fig. 4b). Increasing further the integral gain of the feedback to reduce the offset to the setpoint was found to destabilize the control loop. The film thickness is measured to be 9 Å, and the noise amplitude of $\pm$2 Å visible on Fig. 4c is not affected by shear motion and corresponds to the measurement sensitivity at the chosen acquisition rate. Steady sliding is observed under a shear force of 8 μN (Fig. 4d). In open-loop conditions, *i.e.* without normal load feedback, the non-parallelism of the surfaces (5×10^{-3} rad for this experiment) would yield a load variation of about 15 μN/μm, resulting in a complete loss of confinement after 20 μm of forward shear.

Larger shear amplitudes and lower load levels can readily be achieved. This is illustrated on figure 5, where a load of 21$\pm$3 μN (setpoint 24 μN) is maintained over 400 μm at a sliding speed of 2 μm.s^{-1}.

Experiments can also be performed under low confinement, by using the intersurface distance as the input signal of the feedback control. On figure 6, we show such an experiment where a film of hexadecane is sheared over 250 μm at a velocity of 0.5 μm.s^{-1}, while maintaining its thickness at 60$\pm$1.5 Å(distance setpoint 60 Å). Under these confinement conditions, normal and shear forces are below the instrument resolution.

The maximum acquisition rate of 27 Hz for simultaneous measurement of forces and distance limits the overall performances of the digital feedback loop and the range of accessible sliding speed. Typically, fluctuations of 20–30 μN or 10–20 Å are observed on normal force or distance when using a sliding speed of 20 μm.s^{-1}. No noticeable noise is induced by the feedback control when the sliding velocity stays below 2 μm.s^{-1}.

IV. CONCLUSIONS

We have built a surface force apparatus specially designed for shear experiments over large sliding distances (>100 μm). Feedback control is used in order to keep the normal load or the thickness of the confined medium constant during motion. The instrument exhibits exceptional performances in terms of force or distance stability, even in situations of weak confinement under small or zero applied load. We now plan to use this apparatus to investigate the shear behavior of glassy polymer thin films under low pressure, and more generally of media presenting a complex molecular architecture, where large shear strains are needed in order to establish a steady-state regime.

[1] D. Tabor, R. H. S. Winterton, Proc. R. Soc. London Ser. A **312**, 435 (1969).

[2] J. N. Israelachvili, D. Tabor, Proc. R. Soc. London Ser.

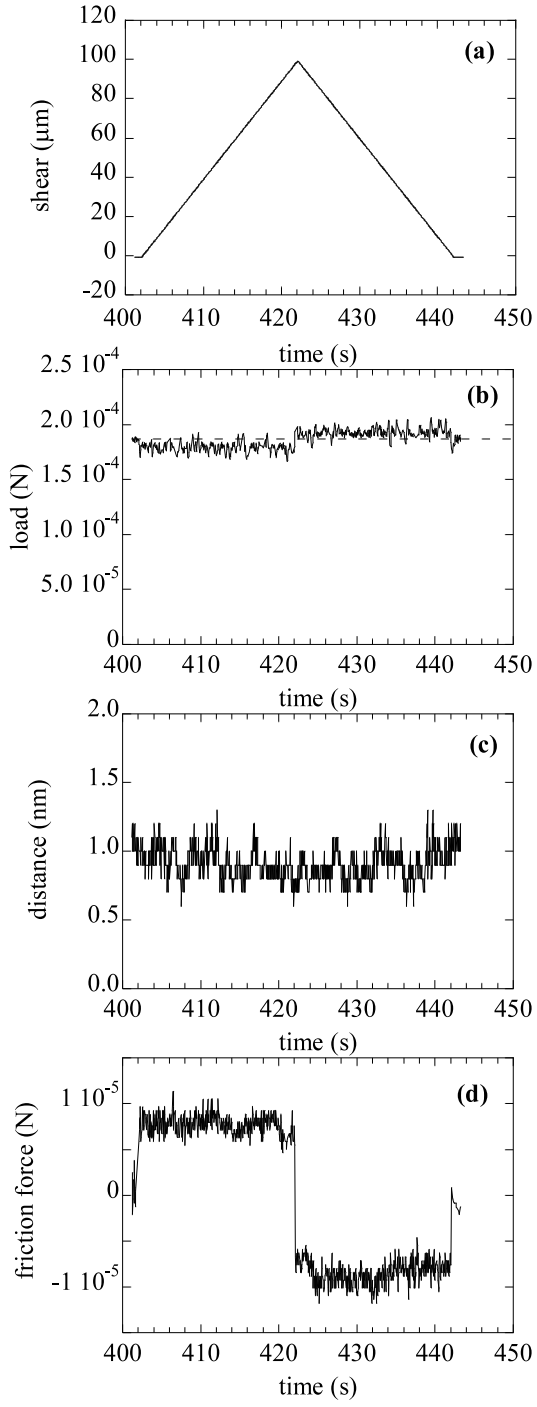

FIG. 4: Friction experiment at controlled normal load over a sliding distance of 100 μm. (a) shear displacement. (b) normal load (the horizontal dashed line indicate the setpoint). (c) distance (the apparent increase/decrease of distance on a 20 s time scale actually corresponds to the point of closest distance moving slightly off-axis of the microscope objective during shear). (d) friction force.

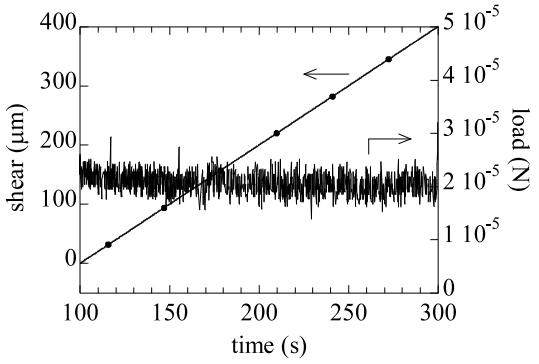

FIG. 5: Shear experiment at controlled normal load over a sliding distance of 400 μm. Left scale: shear motion. Right scale: normal load.

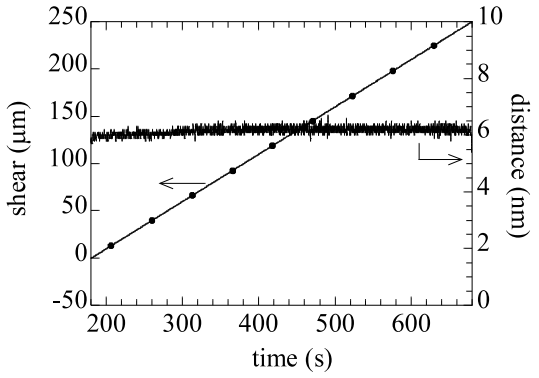

FIG. 6: Shear experiment at controlled intersurface distance over a sliding distance of 250 μm. Left scale: shear motion. Right scale: distance.

A **331**, 19 (1972).
[3] J. N. Israelachvili, G. E. Adams, J. Chem. Soc. Faraday Trans. **74**, 975 (1978).
[4] R. G. Horn, J. N. Israelachvili, Chem. Phys. Lett. **71**, 192 (1980).
[5] J. N. Israelachvili, Intermolecular and Surface Forces, Academic Press (1992).
[6] H.K. Christenson, D. W. R. Gruen, R. G. Horn, J. N. Israelachvili, J. Chem. Phys. **87**, 1834 (1987).
[7] R. G. Horn, J. N. Israelachvili, J. Chem. Phys. **75**, 1400 (1981).
[8] J. Klein, E. Kumacheva, J. Chem. Phys. **108**, 6996 (1998).
[9] Zhu Yingxi, S. Granick, Phys. Rev. Lett. **93**, 096101 (2004).
[10] G. Reiter, A. L. Demirel, S. Granick, Science **263**, 1741 (1994).
[11] J. Peachey, J. Van Alsten, S. Granick, Rev. Sci. Instrum. **62**, 463 (1991).
[12] J. N. Israelachvili, P. M. McGuiggan, A. M. Homola, Science **240**, 189 (1988).
[13] M. L. Gee,P. M. McGuiggan,J. N. Israelachvili,A. M. Homola, J. Chem. Phys. **93**, 1895 (1990).

[14] E. Kumacheva, J. Klein, J. Chem. Phys. **108**, 7010 (1998).
[15] L. M. Qian, G. Luengo, D. Douillet, M. Charlot, X. Dollat, E. Perez, Rev. Sci. Instrum. **72**, 4171 (2001).
[16] P. A. Schorr, T. C. B. Kwan, S. M. Kilbey, E. S. G. Shaqfeh, M. Tirrell, Macromolecules **36**, 389 (2003).
[17] C. Drummond, J. Israelachvili, Macromolecules **33**, 4910 (2000), and references therein.
[18] D. Gourdon, J. Israelachvili, Phys. Rev. E **68**, 021602-1 (2003).
[19] G. Luengo, M. Heuberger, J. Israelachvili, J. Phys. Chem. B **104**, 7944 (2000).
[20] Parker, J.L.; Christenson, H.K.; Ninham, B.W., Rev. Sci. Instrum. **60**, 3135 (1989).
[21] M. Heuberger, Rev. Sci. Instrum. **72**, 1700 (2001).
[22] J. Bechhoefer, Rev. Mod. Phys. **77**, 783 (2005).